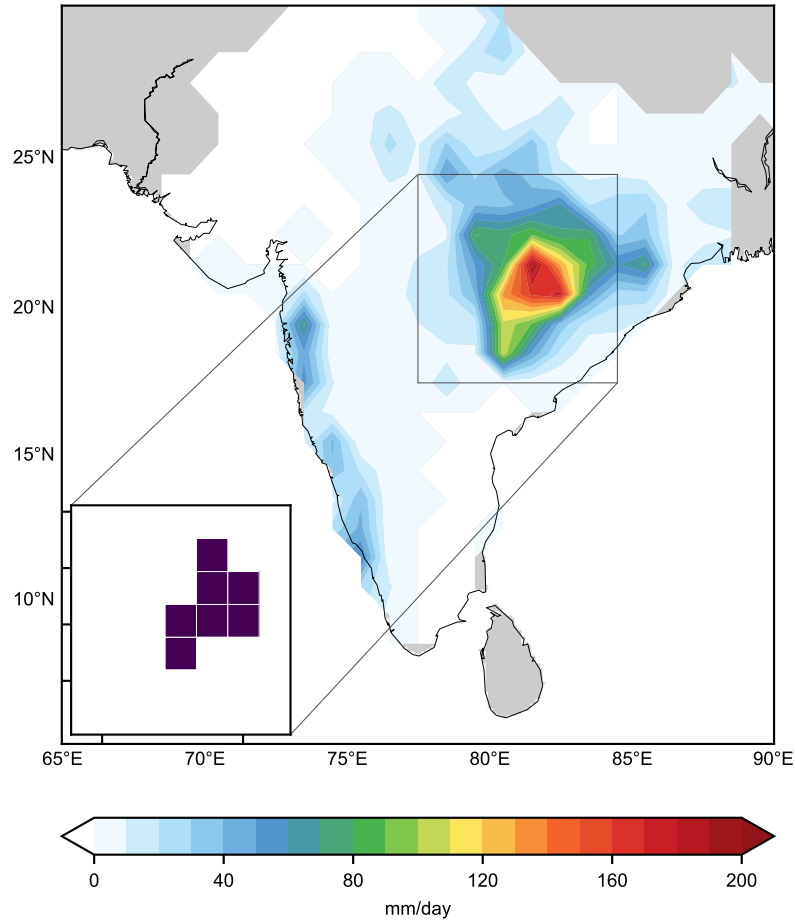


Supplementary Information for "Recent spatial aggregation tendency of rainfall extremes over India"

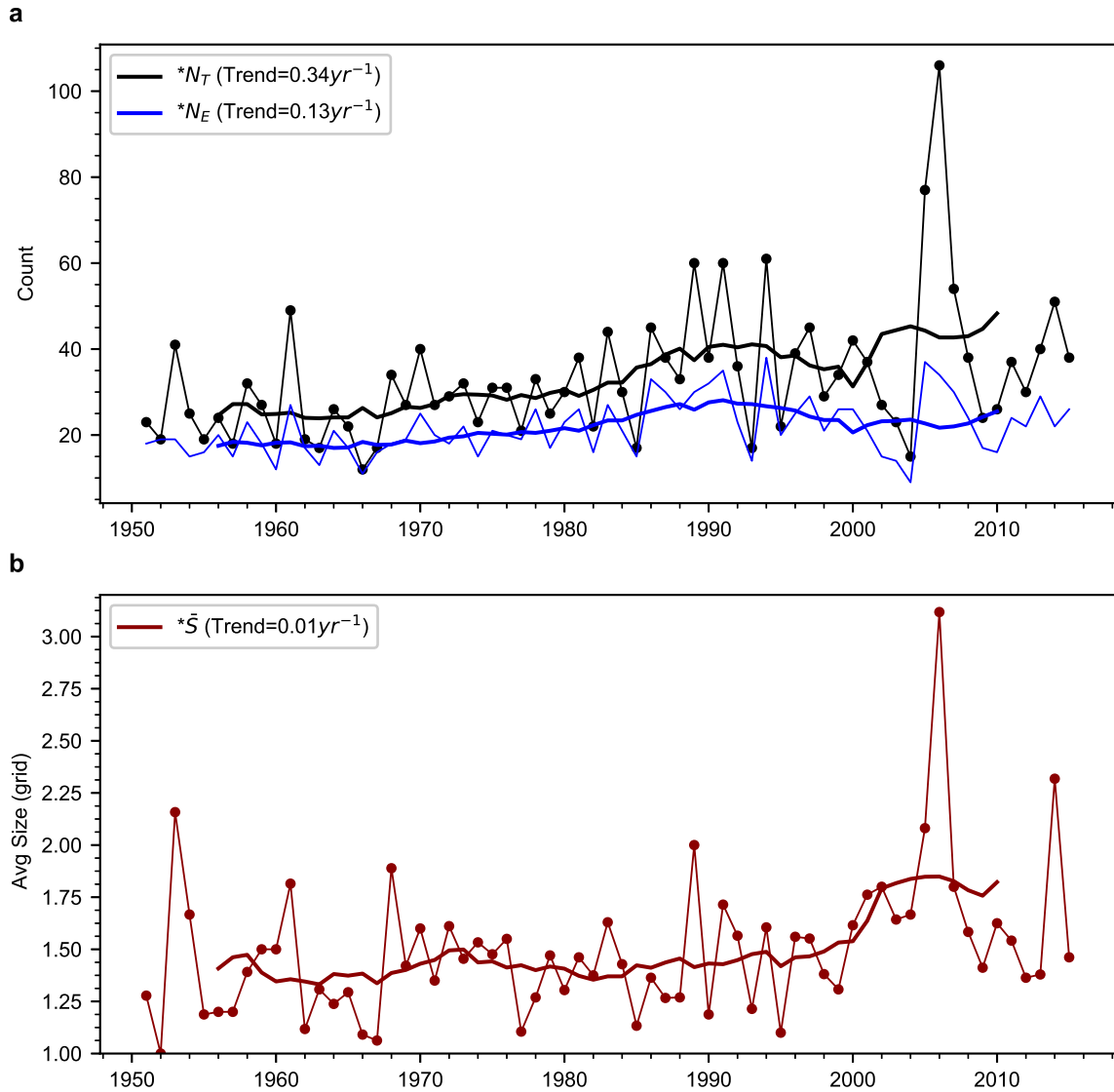
Akshaya C. Nikumbh^{1,2}, Arindam Chakraborty^{1,2*} & G. S. Bhat^{1,2}

¹*Centre for Atmospheric and Oceanic Sciences, Indian Institute of Science, Bangalore, 560012, India.*

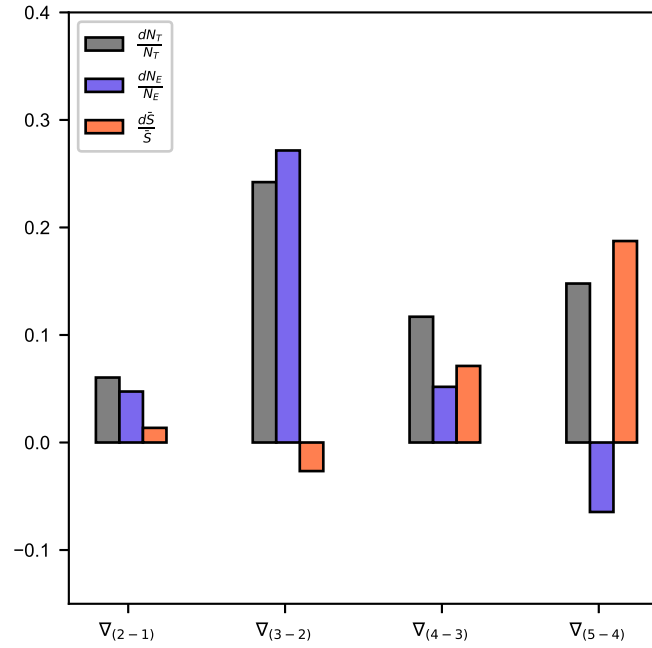
²*Divecha Center for Climate Change, Indian Institute of Science, Bangalore, 560012, India.*



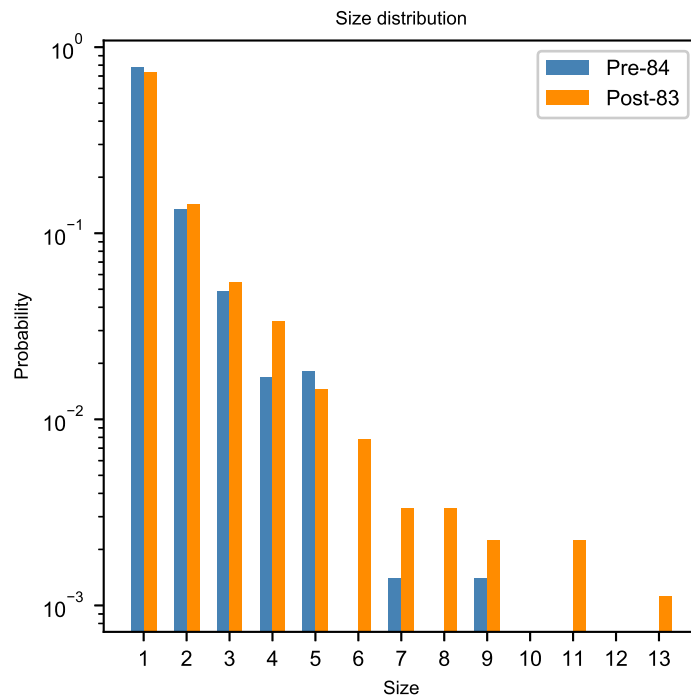
Supplementary Fig. 1. An example of the extreme rainfall event that occurred on 22 July 2014, covers seven $1^\circ \times 1^\circ$ grids. In this study, it is identified as a single event of the size 7 (shown in the inset box) rather than 7 different events by the method used in the past studies. This event contributed 7 and 1 to N_T and N_E , respectively.



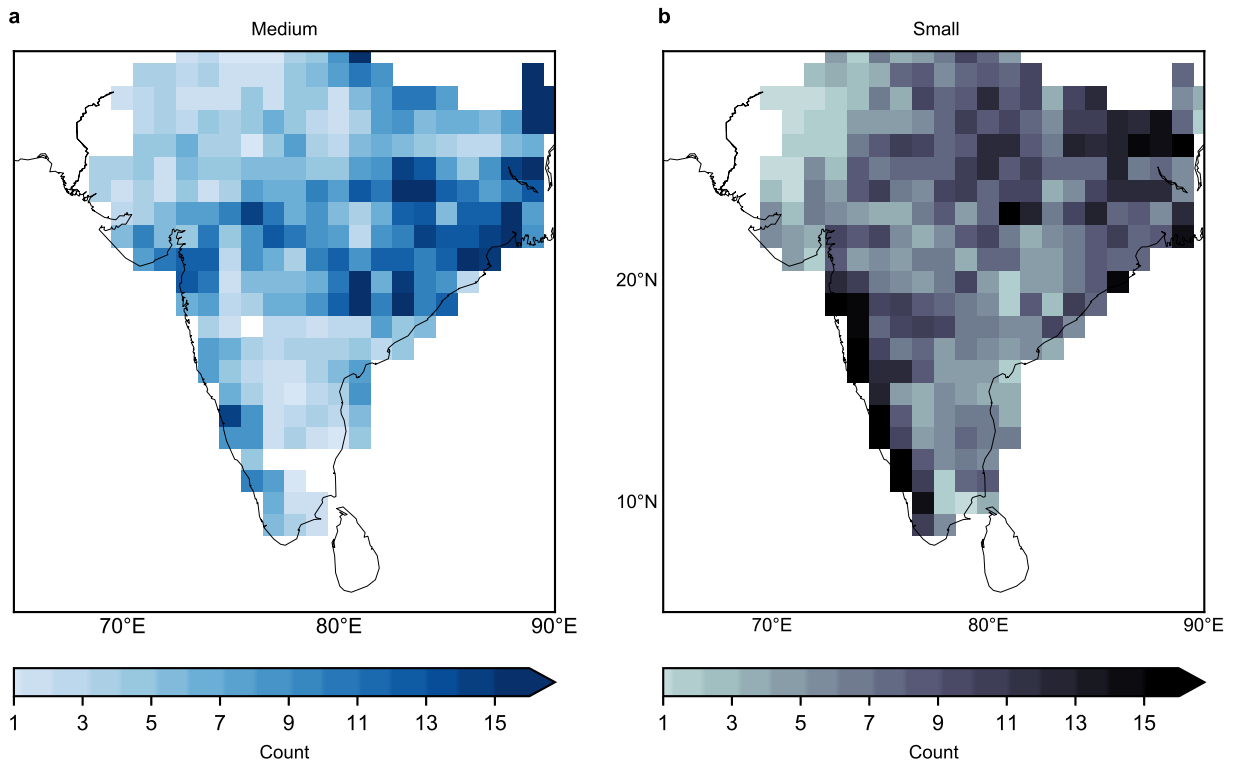
Supplementary Fig. 2. Time series of **a.** the total number of $1^\circ \times 1^\circ$ grids with extreme rainfall (N_T), the number of extreme rainfall events (N_E), and their **b.** average size (\bar{S}) over Central India. The smoothed curves on the time series plots represent 11-year moving averages. Asterisks(*) indicate the increasing trends are significant at the 99% confidence level using the Mann-Kendall test.



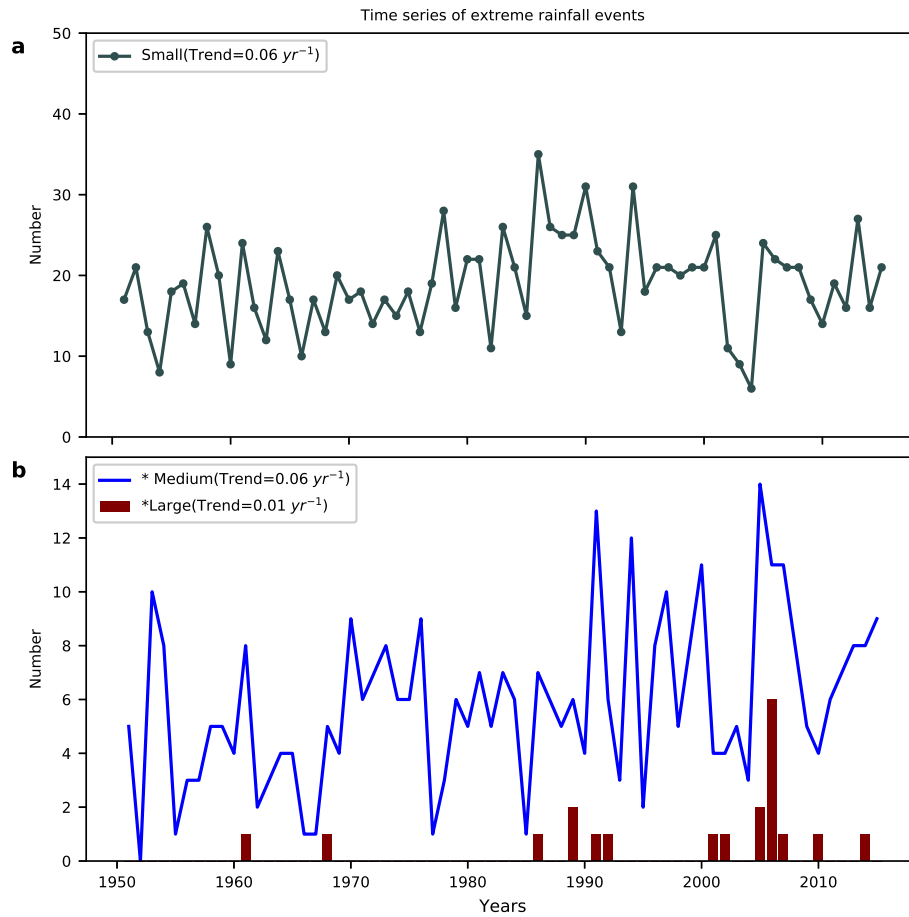
Supplementary Fig. 3. The contribution by fractional changes in the average size ($\frac{d\bar{S}}{\bar{S}}$) and the count ($\frac{dN_E}{N_E}$) to the total number of $1^\circ \times 1^\circ$ grids with extreme rainfall ($\frac{dN_T}{N_T}$) for different sets (m) of years (Sets: 1951-1964, 1964-1977, 1977-1990, 1990-2003, 2003-2015). $\nabla_{(m+1-m)}$ indicates fractional changes calculated from consecutive sets ($m+1, m$) (See method section for details).



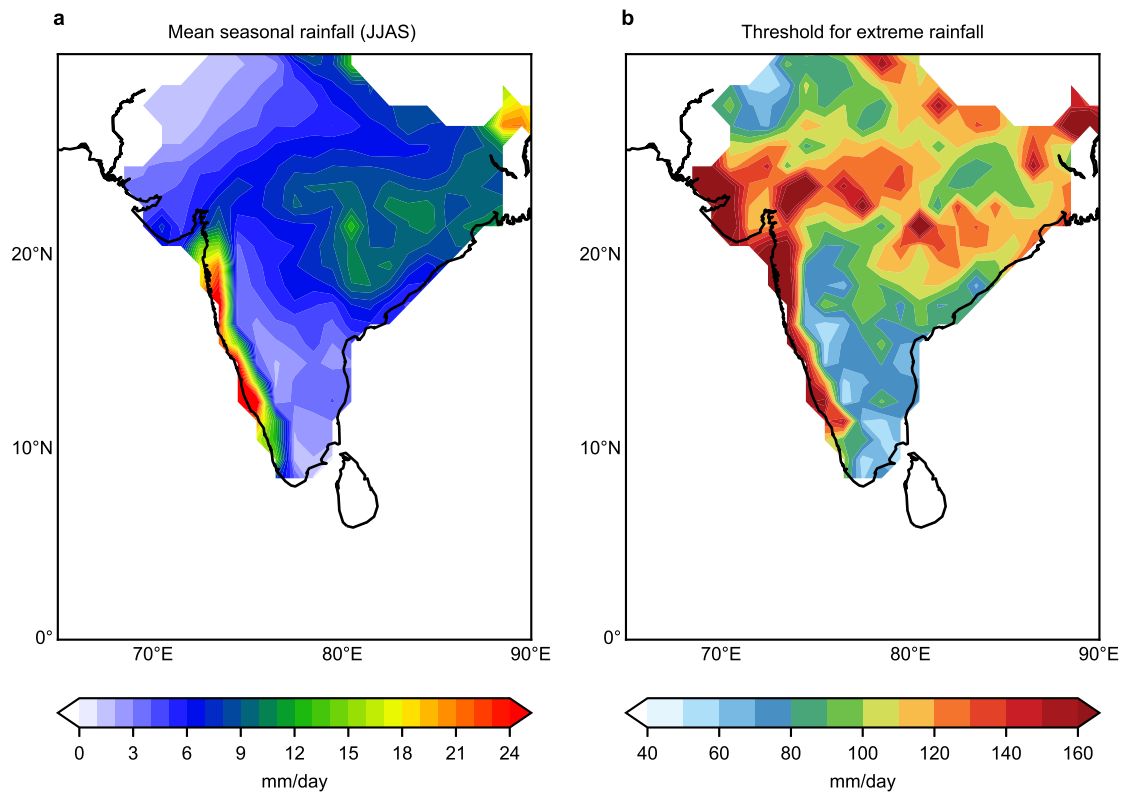
Supplementary Fig. 4. Normalized size distribution of extreme rainfall events during the pre-84 (1952-1983) and post-83 (1984-2015) periods.



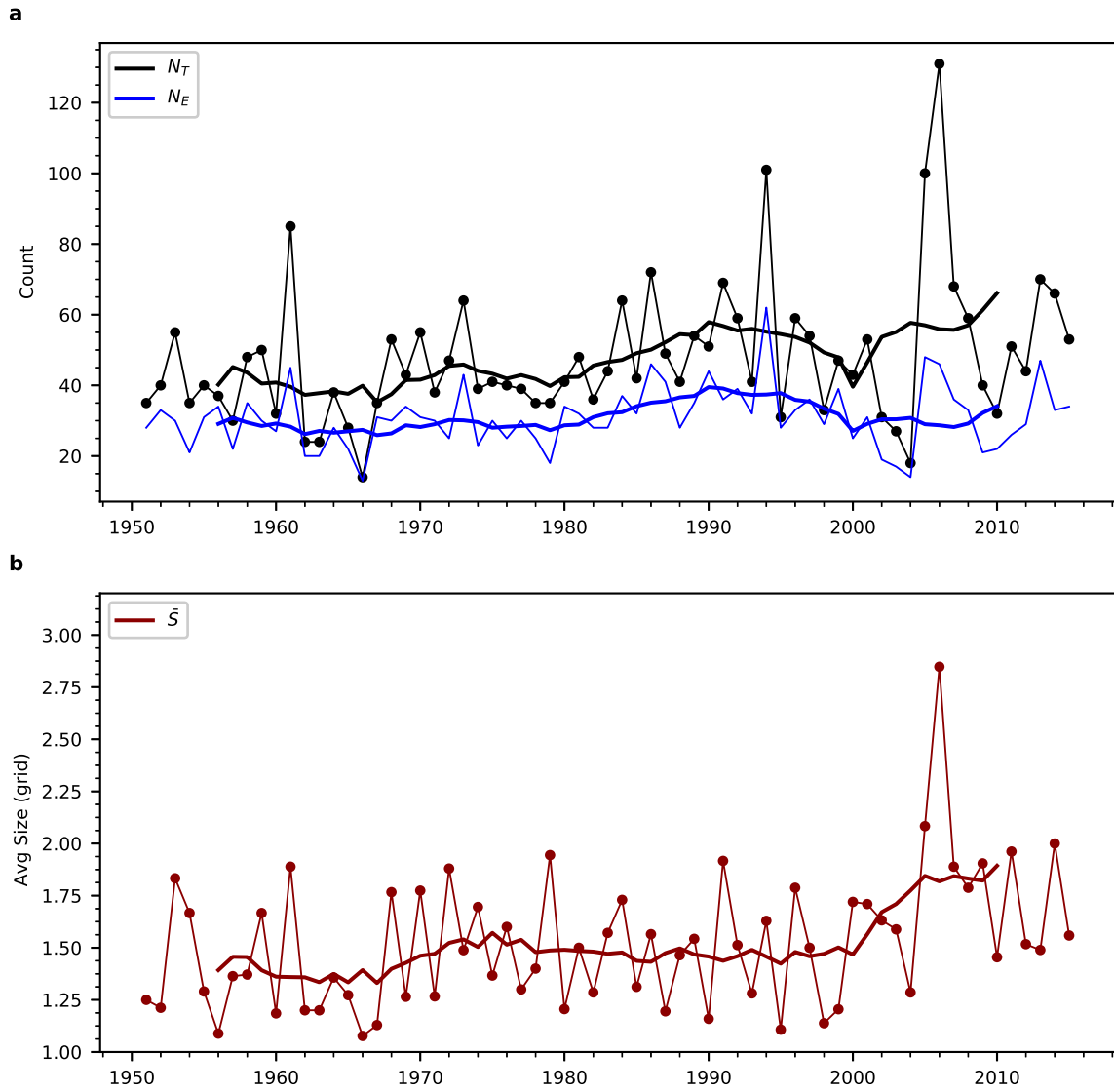
Supplementary Fig. 5. Spatial distribution of **a.** medium and **b.** small extreme rainfall events



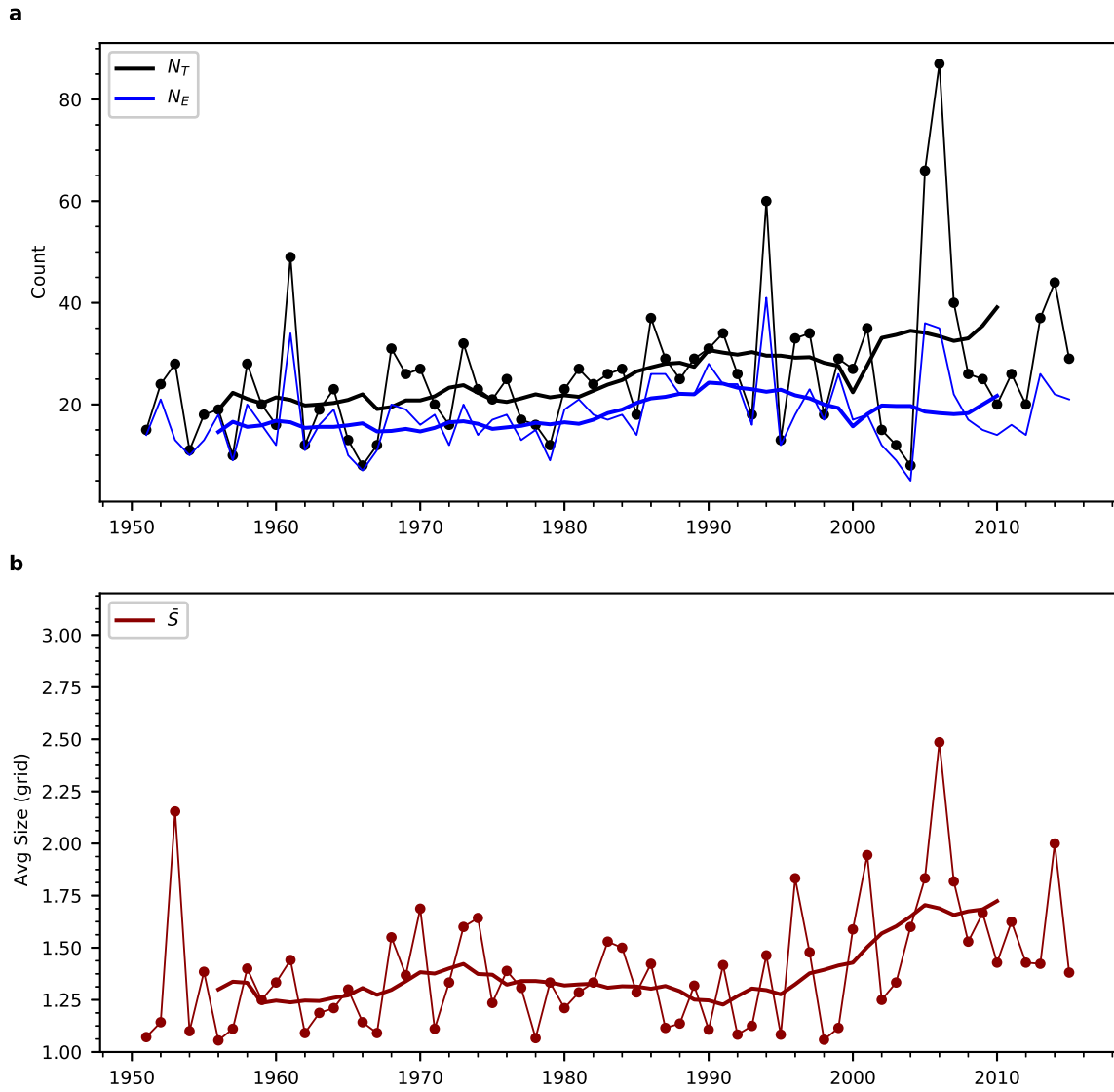
Supplementary Fig. 6. Time series of small, medium and large extreme rainfall events. Asterisks(*) indicate the increasing trends are significant at the 95% confidence level using the Mann-Kendall test.



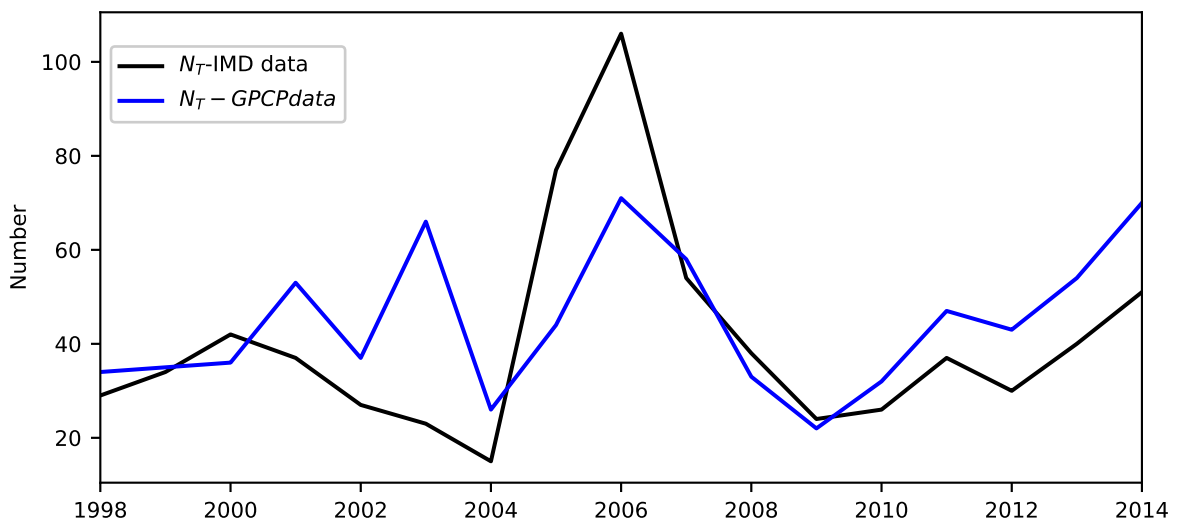
Supplementary Fig. 7. a. Climatology of daily rainfall during the Indian summer monsoon **b.** 99.5th percentile threshold. Both are obtained using JJAS rainfall data for the period 1951-2015.



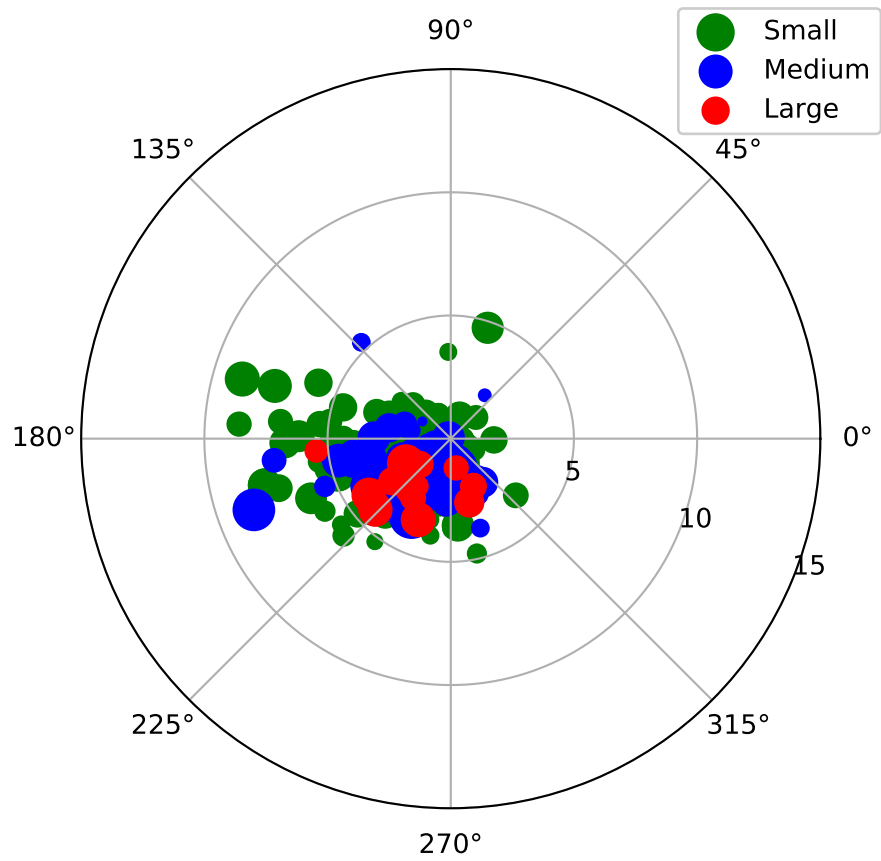
Supplementary Fig. 8. Same as Supplementary Fig. 2. but for a fixed threshold of 100 mm day⁻¹.



Supplementary Fig. 9. Same as Supplementary Fig. 2. but for a fixed threshold of 120 mm day⁻¹.



Supplementary Fig. 10. Time series of N_T using the GPCP 1DD v1.2 dataset and the IMD dataset.



Supplementary Fig. 11. The relative locations of Small, medium and large EREs relative to the Monsoon depression.